METEOROLOGICAL APPLICATIONS
*Meteorol. Appl.* **22**: 617–635 (2015)
Published online 15 April 2015 in Wiley Online Library
(wileyonlinelibrary.com) DOI: 10.1002/met.1497

Royal Meteorological Society

# Some observed characteristics of frontal systems in the Amazon Basin

Alcides de Castro Amorim Neto,[a] Prakki Satyamurty[b]* and Francis Wagner Correia[c]
[a] *CLIAMB, UEA-INPA, Manaus, AM, Brazil*
[b] *CESTU, UEA, Manaus, AM, Brazil*
[c] *EST, UEA, Manaus, AM, Brazil*

**ABSTRACT:** The precipitation and the subsequent decline in temperature at Manaus (3 ° S, 60 ° W) associated with strong cold frontal passages occur 1–3 days after those effects are observed at São Paulo (23 ° S, 46 ° S). The average rainfall of 40.4 mm day$^{-1}$ on the day of frontal passage over the Amazon Basin is substantially higher than that on the preceding and succeeding days. The decline in maximum temperature of about 8 °C in 48 h is much greater than the decline in minimum temperature (3 °C) observed at Manaus. The development of an inverted trough in the lower troposphere over the continent in the subtropics strengthens the southerly winds and makes them reach the Amazon Basin. The extratropical synoptic-scale trough at 925 hPa level, associated with cold front over the Amazon Basin in the South Atlantic moves from 40 ° W to 25 ° W in 2 days. The vertical westward tilt of the anomalous low is about 12 ° longitude from 925 hPa to 200 hPa. The rainfall has no correlation with either the temperature or the decline in temperature associated with fronts in the Amazon Basin. During cold frontal events, especially in winter cases, the transport of moisture from the Amazon Basin to the south is either weak or absent. The differences between winter and summer cases are large in terms of precipitation, temperature, wind anomalies and eastward and northward movements of the synoptic system.

KEY WORDS forecasting; hydro-meteorology

*Received 4 November 2013; Revised 27 October 2014; Accepted 8 December 2014*

## 1. Introduction

The Amazon Basin, situated in the equatorial latitudes of South America, receives on an average about 2200 mm of rainfall annually (Figueroa and Nobre, 1990; Rao *et al.*, 1996; Satyamurty *et al.*, 1998). Both organized and disorganized convections are responsible for the rainfall. Among the meteorological systems that organize convection in the Amazon Basin are instability lines (Cohen *et al.*, 1995), South Atlantic Convergence Zone (SACZ, Kodama, 1993; Figueroa *et al.*, 1995) and cold frontal systems (CFs) migrating from the south (Garreaud and Wallace, 1998). The instability lines develop near the northern coast of South America and, embedded in the equatorial easterlies, propagate westward as far as 2000 km into the interior from the coast. The SACZ is an elongated zone of low-level convergence of moisture extending from the basin into the South Atlantic Ocean that can form over the continent in the period November through March. The SACZ episodes have an average duration of a week (Vieira *et al.* 2012), and during these episodes, the number of heavy rain events is substantially higher than the climatology. The CFs associated with the extratropical baroclinic waves first propagate eastward from the South Pacific into Argentina and then northeastward into Brazil. Garreaud and Wallace (1998) (hereafter referred to as GW) showed that the convective activity associated with frontal incursions into the tropics of South America in austral summer (December, January and February) retains its identity over 5 days. They also affirmed that the mid-latitude system incursions into the tropics are responsible for 50% of the precipitation in summer. Occasionally, the CFs propagate as far north as the Amazon Basin (Fortune and Kousky, 1983; Marengo *et al.*, 1997) with their characteristic effect of causing precipitation and decline in temperature.

For improving the weather forecasts of the Amazon region, it is necessary to improve the knowledge of the CFs in this region and the rainfall and temperature changes caused by the passage of these systems. The present study focuses on these systems affecting the Amazon Basin. This study is undertaken to answer questions regarding the relation between the frontal passages in southern Brazil and in the Amazon Basin, the structures of the wind and temperature fields associated with the Amazon CFs and their contribution to the precipitation of the region. There are some other outstanding questions such as how strong the association is between the precipitation and the subsequent temperature decline caused by cold air advection over the Amazon region. Other important questions are whether the precipitation associated with a frontal passage is significantly different from that associated with the daily convective activity and how strong the moisture convergence associated with the frontal passages over tropical South America is.

The South American subtropics and tropics are one of the exceptional regions of the globe where the cold fronts penetrate deep into the tropics, as far north as 5 ° S, occasionally crossing the equator (Kousky and Ferreira, 1981). That is, the South American continent is a region of strong interaction between the tropics and the extratropics. The frontal effects and the structure of the fronts over the mid-latitudes and the high latitudes are studied widely and are an important topic of several textbooks (e.g. Palmén and Newton, 1969; Bluestein, 1993). However, the structure of the fronts penetrating into the tropics is not commonly found in the literature. The present study addresses

* Correspondence: P. Satyamurty, CPTEC, INPE, Sao Jose dos Campos, SP, CEP: 12.227-010, Brazil. E-mail: saty.prakki@gmail.com

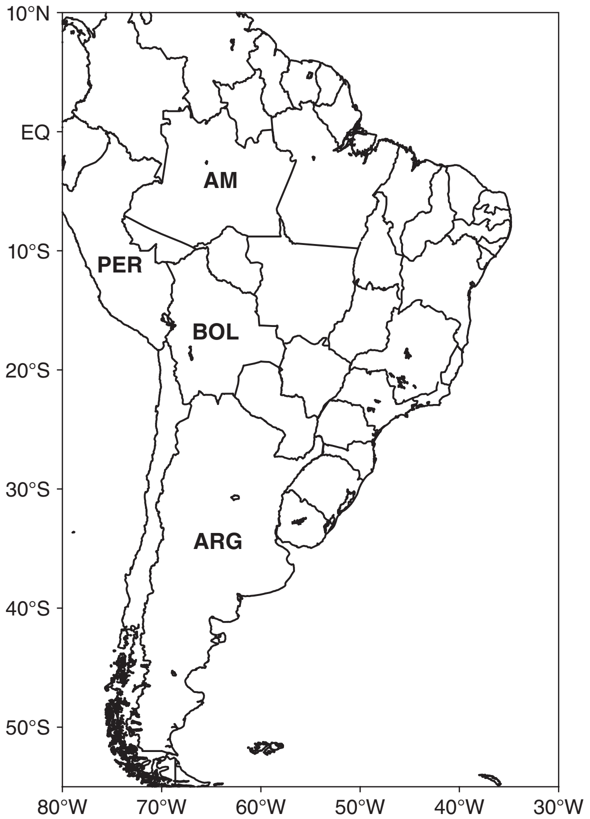


Figure 1. Location map. The three meteorological stations São Paulo, Brasilia and Manaus are shown. AM, state of Amazonas in Brazil; ARG, Argentina; PER, Peru; BOL, Bolivia.

the observational aspects of the cold fronts over the Amazon Basin.

## 2. Data sets

The NCEP/NCAR Reanalysis gridded data at 6 h intervals for the period 2000–2010 with a resolution of 2.5° are used to obtain low-level and upper-level characteristics associated with the frontal systems affecting the Amazon Basin. The CPC/NCEP data sets are used for sourcing gridded precipitation data. The synoptic station data, temperature, precipitation and winds at 12 h intervals and the daily maximum and minimum temperature data at São Paulo (23.5° S, 46.6° W), Brasilia (15.6° S, 47.9° W) and Manaus (3.1° S, 60.0° W) are shown in Figure 1; obtained from the National Institute of Meteorology, these are used to characterize the local variations of the meteorological parameters during the episodes of frontal passage.

## 3. Methodology

First, the frontal systems affecting the Amazon region in the 10 year period 2000–2010 are identified in the monthly bulletins *Climanalise* of the Center for Weather Forecasts and Climate Studies (CPTEC). Second, the GOES IR and VIS images for those cases are examined to verify if a cloud band is present over the Amazon Basin. An example of the northward progression of a cloud band over South America reaching the Amazon region on 5 February 2008 as seen in infrared satellite imagery is presented in Figure 2. Third, the surface temperature data at Manaus are used to verify if the temperature presented a decline of at least 2 °C in 24 h. This criterion is used to eliminate the weak fronts and to consider only those fronts that cause strong temperature changes over the Amazon region. GW have shown a temperature drop in 2 days of about 4.5 °C in winter and about 2 °C in summer in 2 days in the subtropical plains of South America (their Figure 17) taking into consideration all the fronts in the 17 year period studied by them. This prompted the choice of the criterion given above and used in the present study in which the intention is to obtain the characteristics of strong fronts or '*friagens*' in the Amazon Basin as observed in the first decade of the century. In all, 24 cases meeting all the three requirements are identified in the 10 year period of 2000–2010. Of these, 16 occurred in austral winter (May through October) and the rest in austral summer months (November through April).

For the sake of a heuristic discussion of local evolution of precipitation at Manaus, rainfall between 10 and 20 mm in a day is considered moderate, between 20 and 40 mm is considered intense and above 40 mm is considered heavy.

The NCEP/NCAR reanalysis gridded data with 2.5° latitude and 2.5° longitude resolution are used to describe the temperature, precipitation and wind distribution associated with the CFs, during the 3 days $d-1$, $d$ and $d+1$. Here $d$ is the day of occurrence (passage of cold front) at Manaus, and $d-1$ and $d+1$ are the preceding and the succeeding days, respectively. Manaus is chosen to represent the central Amazon Basin because the surface synoptic data at this station are reliable and available with very few missing observations.

The vorticity at 850 and 200 hPa and the vertically integrated convergence of moisture flux are calculated following Satyamurty *et al.* (2013). The integration is performed at the mandatory levels between 1000 and 300 hPa.

The precipitation, surface temperature and lower tropospheric (925 and 850 hPa) and upper tropospheric (200 hPa) winds and all other fields are composited for summer and winter cases for $d-1$ (1 day before the event), $d$ (the day of the event) and $d+1$ (1 day after the event). A 40 year climatology of meteorological fields (Satyamurty *et al.*, 2013) is used to obtain the anomaly fields. The time evolutions of the composite meteorological fields over the South American tropics and subtropics from $d-1$ to $d+1$ are discussed. The evolution of the minimum and maximum temperatures, precipitation and surface pressure at Manaus are compared with those at São Paulo and Brasilia situated south of the Amazon Basin, for the two distinct cases.

## 4. Results

### 4.1. Meteorological variables and fields associated with fronts over the Amazon Basin

The dates of occurrence for the 24 cases of strong cold fronts identified over the Amazon Basin during the period 2000–2010 and the associated precipitations and temperatures are given in Table 1. The 16 cases shown in bold occurred in austral winter and the rest (8 cases) in austral summer. The smaller number of strong cold fronts in summer is due to the uniform criterion in terms of temperature decline used for both the seasons.

The mean precipitation at Manaus on day $d$ is 40.4 mm, which is seven times higher than the mean precipitation 1 day before ($d-1$) and 1 day after ($d+1$) the event (5.6 mm), and is more than six times higher than the annual mean daily precipitation of about 6 mm day$^{-1}$. Therefore, the effect of the cold front on the temporal variability of precipitation in the Amazon Basin is undoubtedly significant. It is interesting to know that

 

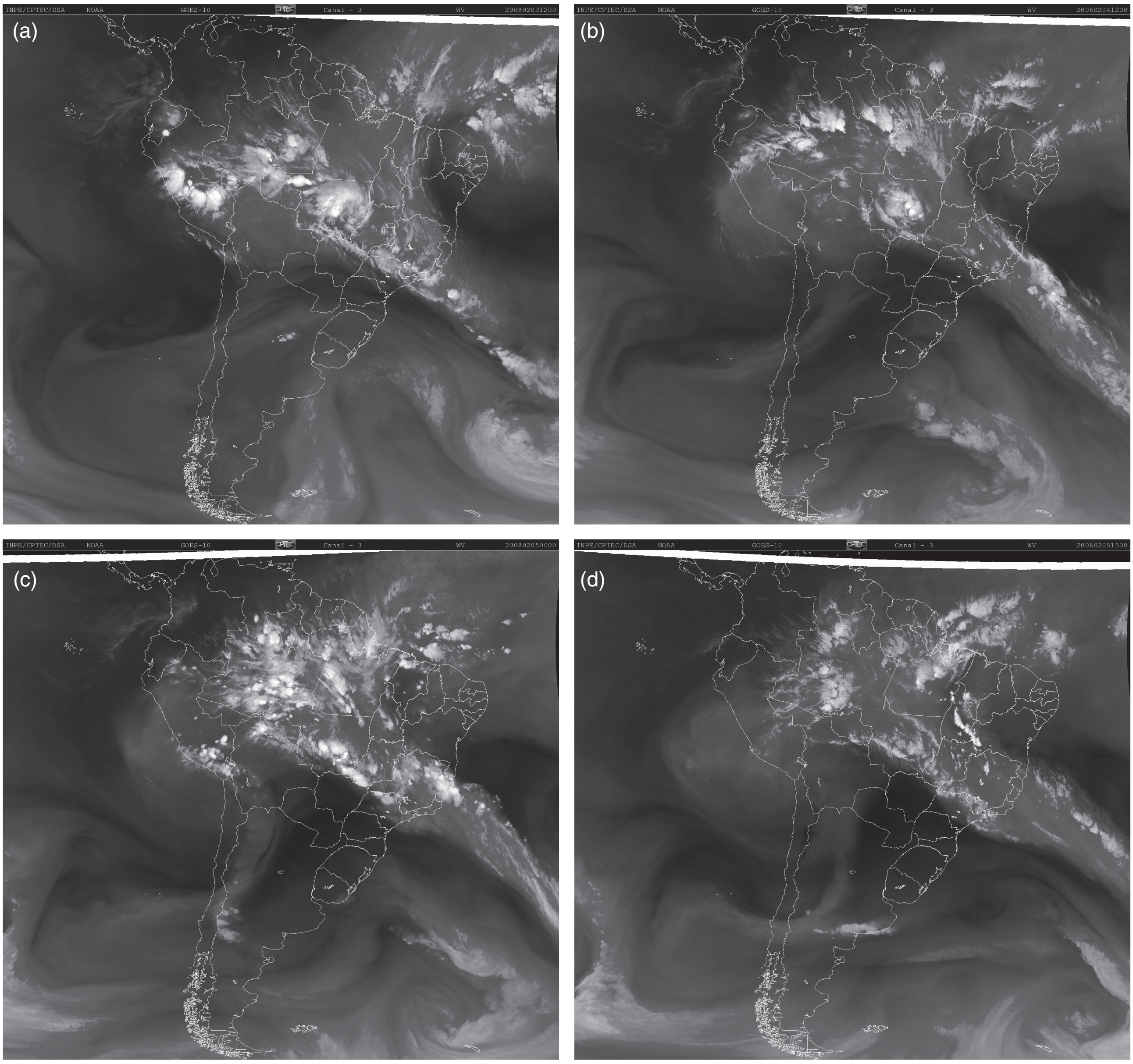


Figure 2. GOES IR image for (a) 1200 UTC on 3 February 2008, (b) 1200 UTC on 4 February 2008, (c) 0000 UTC on 5 February 2008 and (d) 1500 UTC on 5 February 2008. Bright areas are recognized as towering convection.

the average precipitation of the 16 austral winter cases on day *d* is 35 mm and that the summer cases produced more intense precipitation of 48.5 mm. This is explicable because the temperature and the specific humidity in the Amazon Basin are higher and the convective activity is much more vigorous in summer than in austral winter. Another important observation is that the amount of rainfall the fronts produce is highly variable, being only 13.8 mm day$^{-1}$ for case 8 but 90.8 mm day$^{-1}$ for case 4 (see Table 1). The most rainy cold front case at Manaus occurred in midsummer and the least rainy case in midwinter.

Figure 3 shows the composite distribution of precipitation for the 16 winter cases of CF along with the winter climatology and the anomaly on day *d*. In the northern Amazon Basin, the precipitation exceeded 15 mm day$^{-1}$ in the composite (Figure 3(b)), whereas it is about 9 mm day$^{-1}$ in the climatology (Figure 3(a)). The anomaly around Manaus is stronger than 15 mm day$^{-1}$ (Figure 3(c)). The surface temperature climatology, composite and anomaly distributions are shown in Figure 4. The cold anomaly south of 12 °S is stronger than −3.5 °C. The cold air mass is situated between 12 and 28 °S west of 50 °W. Over the Amazon Basin, the anomalies are weaker; however, over the southern parts of the basin, the anomalies reach −3 °C. That is, the decline of temperature, with respect to the climatological value, during the frontal events is substantial. These events are locally called 'friagens' (Marengo *et al.*, 1997; Satyamurty *et al.*, 1998). The mean frontal boundaries run from 8 °S, 70 °W to 18 °S, 50 °W over the continent. In Figure 4(b), this boundary is located along the southern edge of the yellow shade (23 °C isotherm). The composite fields are tested for statistical significance by applying the Student's *t*-test. For the precipitation composites, the sample is 16, the standard deviation is 4.1 mm and the mean of 15 mm is significant at 95% confidence level. The surface temperature composite value is also significant at the same level of confidence.

 

Table 1. Precipitation and temperature at Manaus during cold frontal episodes.

| Case | Date | Precipitation (mm) | | | Temperature (°C) | | | |
|---|---|---|---|---|---|---|---|---|
| | | *d* | *d* − *1* | *d* + *1* | $\overline{T}$ | *T* | *T* − *1* | *T* + *1* |
| 1 | 15/11/00 | 74.2 | 0.0 | 0.0 | 24.1 | 24.1 | 26.2 | 24.5 |
| **2** | **06/05/01** | **19.6** | **0.0** | **0.8** | **24.1** | **23.5** | **25.6** | **23.6** |
| **3** | **25/05/02** | **29.3** | **4.0** | **11.2** | **24.1** | **23.7** | **26.1** | **24.1** |
| 4 | 10/12/02 | 90.8 | 1.6 | 1.2 | 24.2 | 23.8 | 25.9 | 24.0 |
| 5 | 15/04/03 | 50.6 | 30.2 | 0.0 | 23.9 | 23.3 | 25.3 | 23.6 |
| **6** | **02/05/03** | **30.8** | **14.7** | **18.4** | **24.5** | **23.3** | **25.6** | **23.4** |
| **7** | **07/05/03** | **28.4** | **1.2** | **2.8** | **24.5** | **24.2** | **26.5** | **24.5** |
| **8** | **07/06/03** | **13.8** | **0.0** | **6.6** | **23.6** | **22.3** | **24.7** | **23.0** |
| **9** | **09/08/04** | **55.8** | **0.0** | **2.9** | **24.8** | **22.3** | **24.5** | **22.4** |
| **10** | **12/08/04** | **47.9** | **0.0** | **0.0** | **24.8** | **24.2** | **26.8** | **24.5** |
| **11** | **11/09/04** | **42.1** | **6.0** | **19.4** | **23.6** | **23.7** | **26.0** | **23.9** |
| 12 | 27/12/04 | 50.2 | 0.8 | 0.0 | 23.5 | 23.4 | 25.5 | 23.5 |
| 13 | 28/04/05 | 64.8 | 43.3 | 0.4 | 24.0 | 23.3 | 25.5 | 23.4 |
| **14** | **04/05/06** | **47.8** | **32.0** | **0.0** | **23.5** | **23.4** | **26.0** | **23.7** |
| **15** | **09/05/06** | **77.2** | **0.6** | **8.3** | **23.5** | **23.0** | **25.1** | **23.5** |
| **16** | **30/07/06** | **30.0** | **0.0** | **15.4** | **24.1** | **23.8** | **26.2** | **24.0** |
| **17** | **25/05/07** | **25.0** | **0.0** | **0.0** | **23.8** | **23.0** | **25.3** | **23.8** |
| **18** | **28/07/07** | **41.4** | **0.0** | **4.0** | **24.3** | **24.3** | **26.6** | **24.5** |
| **19** | **28/09/07** | **27.4** | **0.0** | **0.0** | **23.7** | **22.7** | **24.8** | **23.1** |
| 20 | 04/02/08 | 13.4 | No inf. | No inf. | 24.1 | 24.0 | 26.2 | 24.0 |
| 21 | 02/04/08 | 18.0 | No inf. | No inf. | 24.3 | 24.2 | 26.5 | 25.0 |
| 22 | 30/04/09 | 27.4 | 0.0 | No inf. | 24.0 | 24.0 | 26.7 | 24.3 |
| **23** | **01/06/09** | **28.6** | **3.2** | **2.2** | **23.9** | **23.2** | **25.8** | **23.8** |
| **24** | **17/07/10** | **13.9** | **11.6** | **0.0** | **23.9** | **23.5** | **25.5** | **23.6** |
| **Mean** | | **40.4** | **6.8** | **4.5** | **24.0** | **23.5** | **25.8** | **23.8** |

*d* is the day when the front is situated over the Amazon Basin, *d* − 1 and *d* + 1 are the day before and the day after *d*, respectively. The winter events are in boldface. $\overline{T}$ is the mean monthly climatological temperature. *T*, *T* − *1* and *T* + *1* are the minimum temperatures on *d* − 1, *d* and *d* + 1, respectively. Missing information is indicated by 'No inf'.

The lower tropospheric winds are represented here by the winds at 850 hPa. The composites and their anomalies on day *d* for the winter cases are shown in Figure 5 along with the moisture convergence. The climatology presents northerly winds east of the Andes and south of 12 ° S. The composites (Figure 5(b)) show southwesterly winds in the central parts of the continent. That is, when the cold front reaches the Amazon Basin, the winds in the cold air mass have a southerly component and the winds turn cyclonic around the frontal boundary at 850 hPa in the South Atlantic. The equatorial easterlies north of 4 ° S weaken slightly; however, the convergence of moisture over the Amazon Basin is stronger in the composites (Figure 5(b)) than in the climatology (Figure 5(a)), essential for intense rainfall. This is reflected in the anomalies (Figure 5(c)).

Figure 6 shows the composites and the anomalies of the 925 hPa winds for *d* − 1, *d* and *d* + 1 for the winter cases. The anticyclone over Argentina and the trough to its movement eastward from *d* − 1 to *d* + 1 at a speed of ~6 ° longitude day$^{-1}$. The trough associated with CF is at 35 ° W south of 25 ° S in the South Atlantic (Figure 6(b)). Northwest of the trough, the southeasterly winds advect cold air northwestward into the Amazon Basin and cause the temperature to decline. The wind anomalies show a closed cyclonic centre at 33 ° S, 33 ° W and strong winds from southeast to northwest with a long fetch into the southern Amazon Basin (Figure 6(e)). The upper tropospheric winds (200 hPa) on days *d* − 1, *d* and *d* + 1 and their anomalies are shown in Figure 7. The winds are weak in the equatorial latitudes at and north of 5 ° S. South of 15 ° S, the winds are basically westerly. In the anomalies associated with

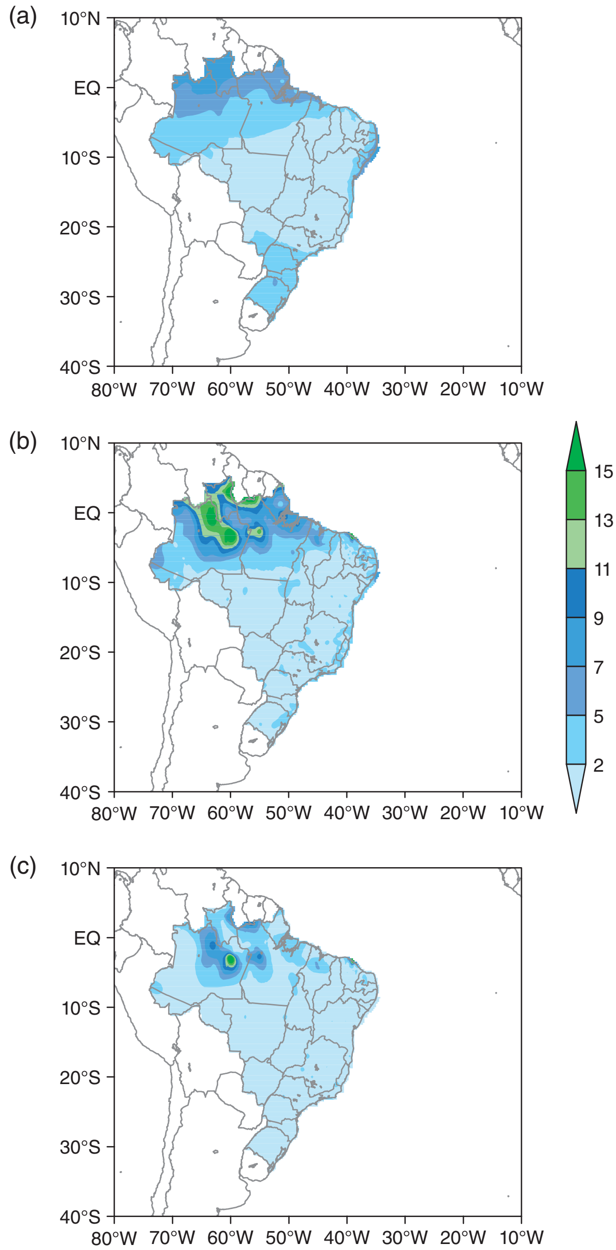


Figure 3. Precipitation (mm day$^{-1}$) over Brazil. (a) Climatology, (b) composite of 16 winter cold front events over the Amazon Basin on day *d* and (c) anomaly.

cold fronts, a strong cyclonic circulation can be seen over and adjacent to South Brazil (Figure 7(d-f)). The westward vertical tilt of the cyclonic centre in the vertical of about 12 ° from the 925 hPa level to the 200 hPa level (compare Figures 6(e) and 7(e)) indicates the existence of a cold air mass over Argentina to the west of the low-level trough anomaly. The wind anomalies in the upper troposphere are northerly over and east of the Andes from 8 to 25 ° S west of 60 ° W. Southerly anomalies in the lower troposphere and northerly anomalies in the upper troposphere indicate strengthening of regional Hadley Cell circulation over the western parts of South American tropics and subtropics in the winter frontal situations over the Amazon Basin due to the increased meridional thermal gradient. There is an anticyclonic anomaly east of the northerlies and north of the anomalous cyclone in the upper troposphere. The anomalous cyclonic circulation in the lower troposphere and an

 

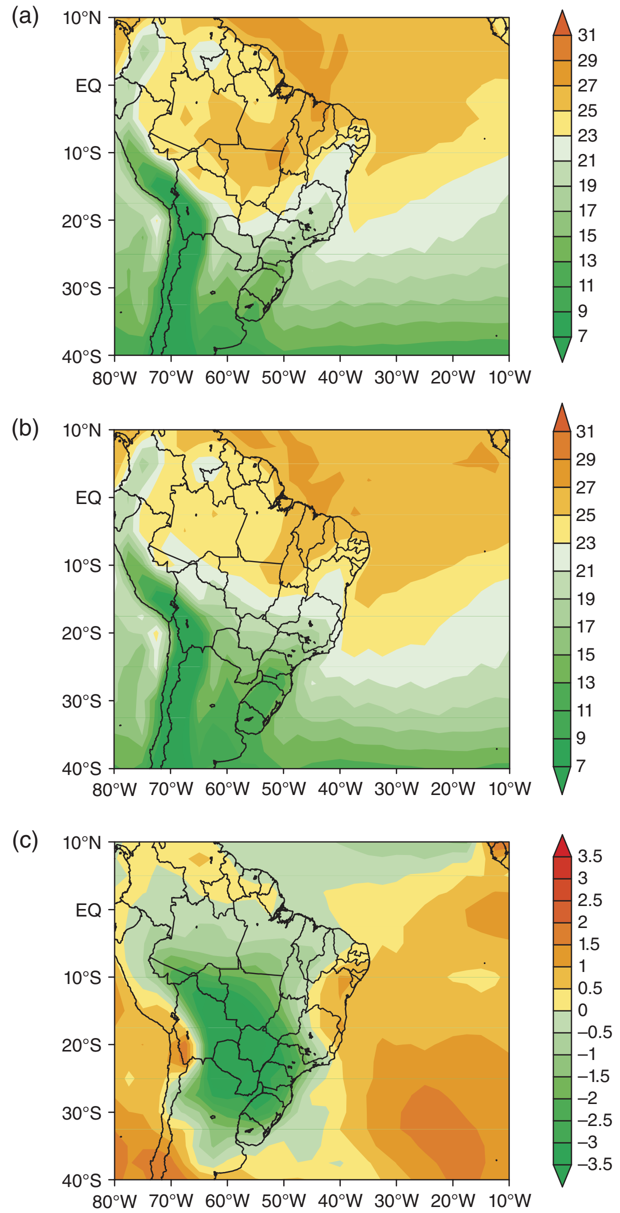


Figure 4. Temperature (°C) at 1200 UTC over South America. (a) Climatology, (b) composite of 16 winter cold front events over the Amazon Basin on day *d* and (c) anomaly.

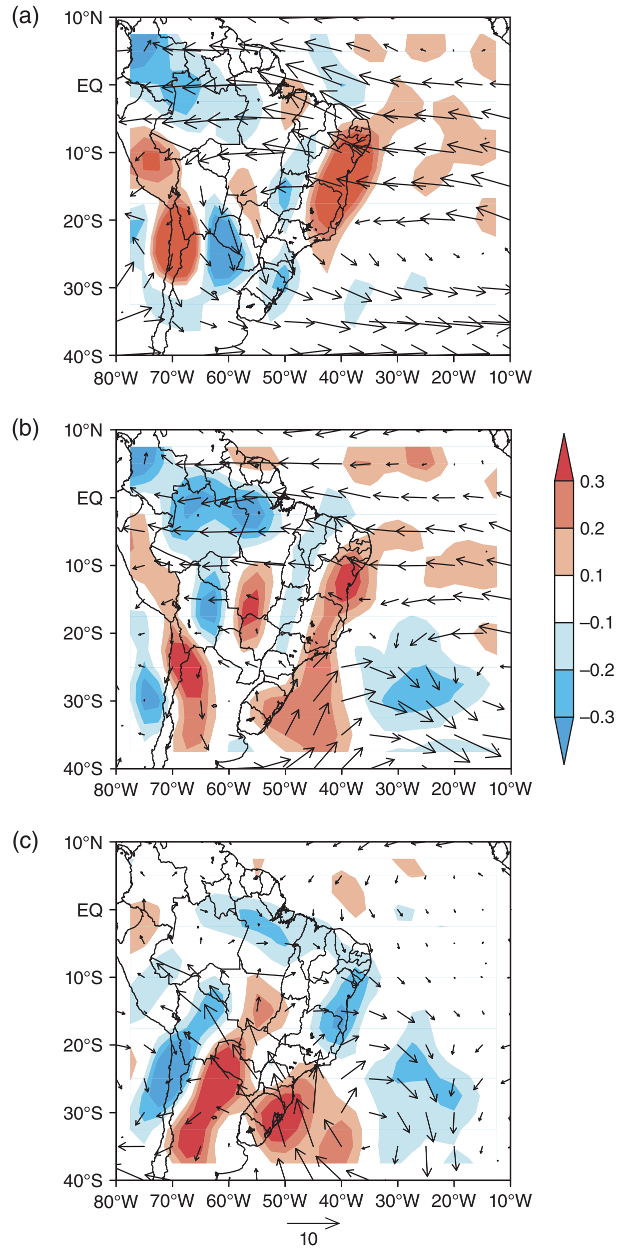


Figure 5. Winds (arrows) in m s$^{-1}$ and moisture convergence (shaded) in $10^{-7}$ s$^{-1}$ at 850 hPa. (a) Climatology, (b) composite of 16 winter cold front events over the Amazon Basin on day *d* and (c) anomaly. Blue: convergence; Red: divergence.

anticyclonic anomaly in the upper troposphere indicate warm air characteristics between 7 and 20 ° S and 60 and 45 ° W in the midtroposphere.

Figure 8 shows the vorticity anomalies in the lower and upper tropospheres for the winter cases. The cyclonic vorticity at the 850 hPa level associated with the front (Figure 8(a)) extends from the South Atlantic Ocean northwestward into the Amazon Basin. The anticyclonic anomaly band in the upper troposphere (Figure 8(b)) is situated almost right over the low-level cyclonic anomaly, which shows the presence of warm air in the midtroposphere as is mentioned in the previous section. That is, although the cold air penetrated into the Amazon Basin near the surface, the midtroposphere remains warm. This makes the layer very stable. This situation is propitious for clear air turbulence. Ahead of the 850 hPa cyclonic zone, in the warm air sector, the convective activity is strong as indicated by the precipitation composite in Figure 3(b).

Figure 9 shows the composites of the vertically integrated moisture flux and its convergence for the winter cases. The similarity between the moisture fluxes (Figure 9(b)) and the lower tropospheric winds (Figure 5(b) and Figure 6(b)) is remarkable, suggesting that the lower tropospheric winds are largely responsible for the moisture fluxes. In climatology (Figure 9(a)), there is a strong southward and southeastward flux from the southern portions of the Amazon Basin into southern and southeastern Brazil as was observed by Nogués-Paegle and Mo (1987). In the cold front composites, this flux is either absent or is very weak. As the southward moisture flux is related to the low-level jet (LLJ, Salio *et al.*, 2002), it can be deduced that the LLJ was either absent or weak over Bolivia and the adjacent regions when the front lies over the Amazon Basin. The anomaly in Figure 9(c) shows a strong southerly to southeasterly component

 

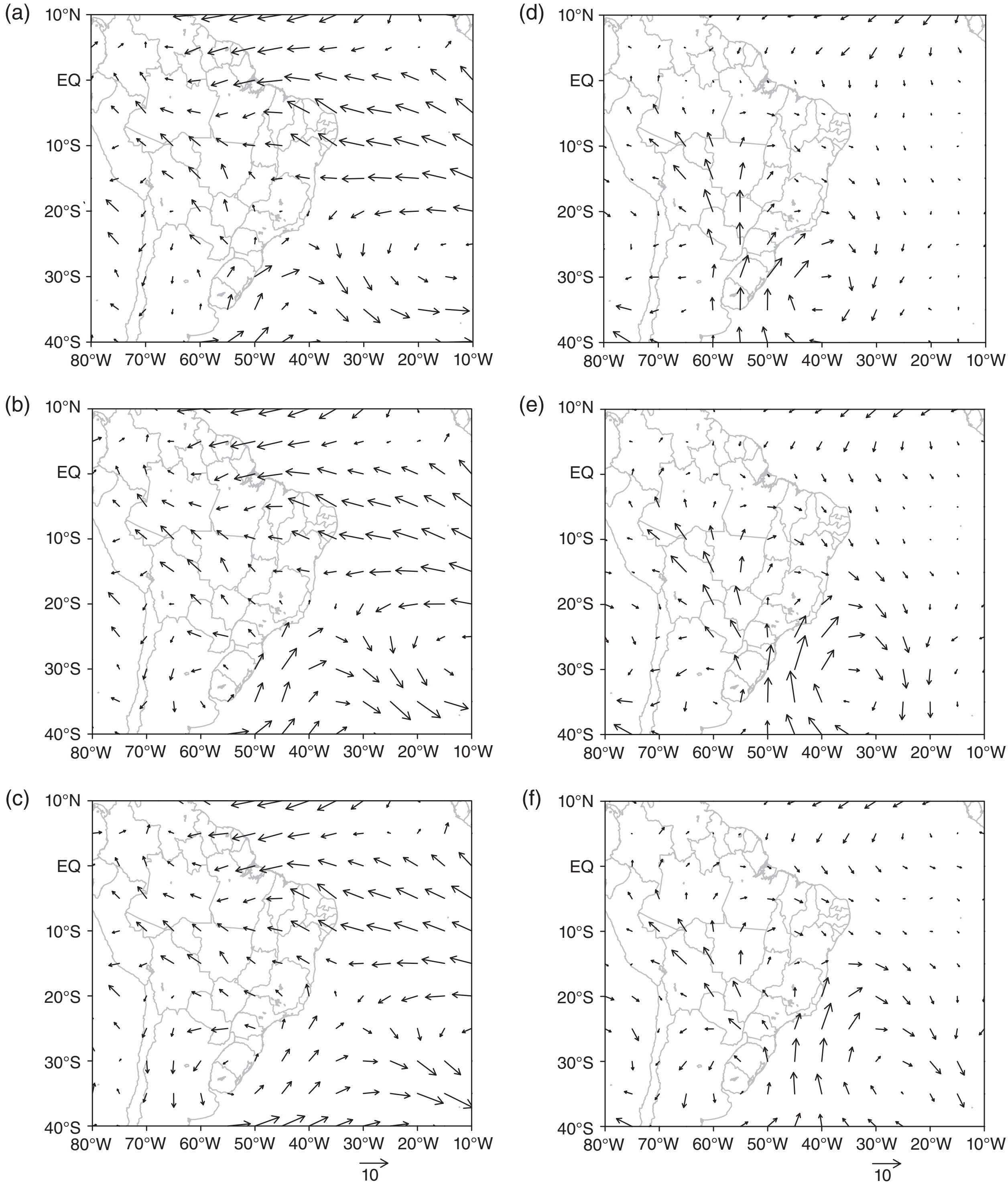


Figure 6. Sequence of 925 hPa wind (m $s^{-1}$) composites (a–c) and anomalies (d–f) on $d-1$ (a and d), $d$ (b and e) and $d+1$ (c and f), for 16 winter cold front events over the Amazon Basin.

of moisture flux into the Amazon Basin. As the southward transport of moisture from the basin is weakened or is absent, the moisture convergence over the basin is strengthened by the easterlies.

Some of the salient features of the summer CF events are shown in Figures 10, 11 and 12. The temperature anomalies (compare Figures 10(c) and 4(c)) are comparable to the winter cases because the criterion used for their identification is the same in both the seasons. The precipitation anomaly over the Amazon Basin associated with the summer CFs (not shown) is similar to that with the winter cases, except it is stronger in the winter CFs. The differences, in the moisture transport (flux) and its convergence, between the two seasons are large. In summer, the convergence is more intense almost over the entire Amazon Basin (Figure 11), which is reflected in the rainfall anomalies. The climatology of moisture convergence is also more intense in summer and, therefore, the anomaly fields are not very different in the two seasons. The vorticity

 

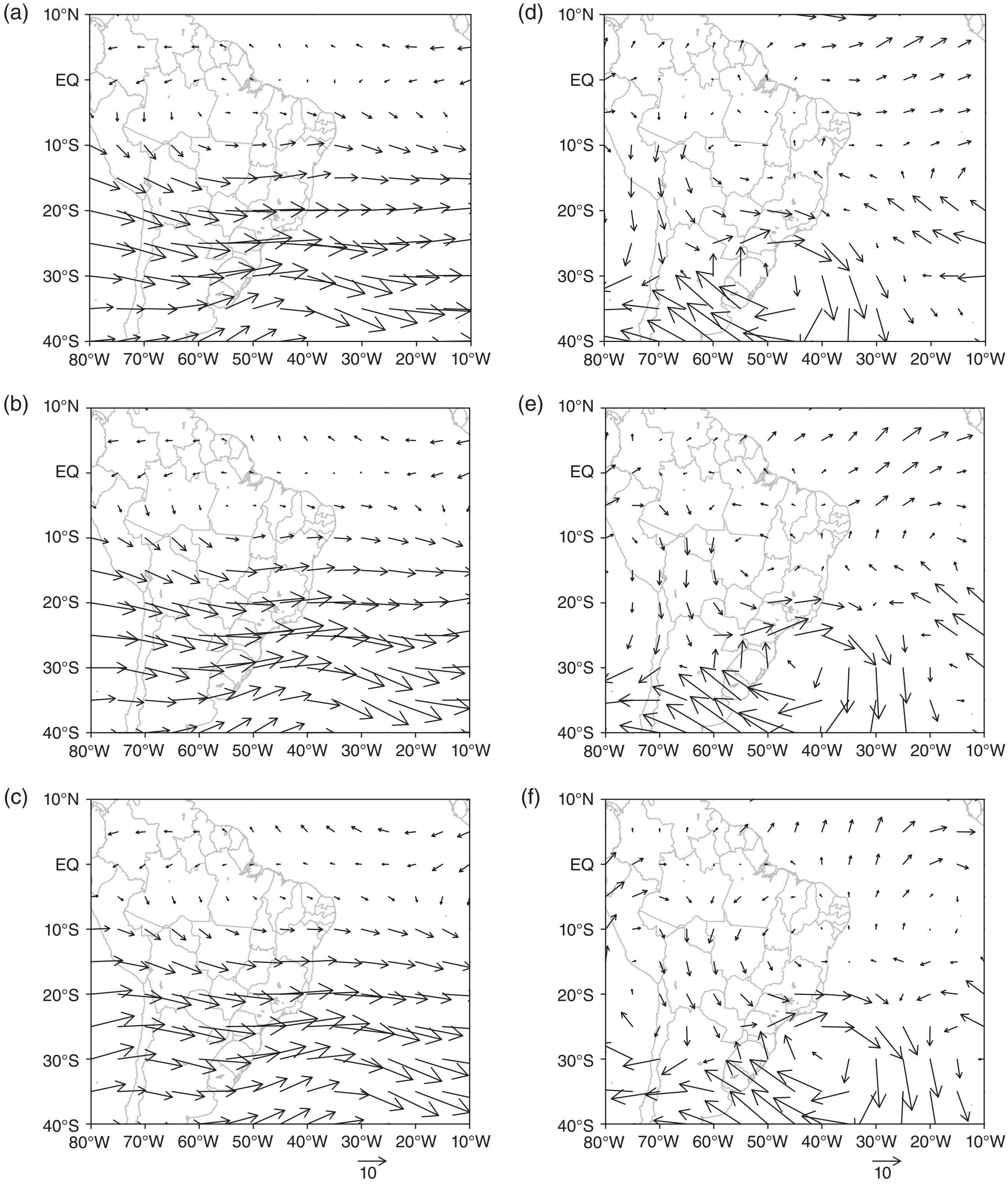


Figure 7. Same as in Figure 6 except for 200 hPa.

fields in the lower and upper tropospheres also show large differences between winter (Figure 8) and summer (Figure 12). The cyclonic vorticity in the lower troposphere (blue shade) in summer is not a continuous band from the Amazon Basin into the South Atlantic Ocean as is the case in winter. However, the surface frontal position can be recognized from the surface temperature composites as shown in Figure 10. The upper tropospheric anticyclonic vorticity anomaly is stronger in summer (Figure 12(b)) than in winter (Figure 8(b)) over the east coast of Brazil. Considering that the most dominant climatological feature in summer is the Bolivian High, Figure 12(b) indicates that in a frontal situation, the anticyclonic area normally centred over Bolivia transforms into an elongated region with greater intensity over the eastern parts of the continent. The subtropical jetstream (not shown) is strengthened around 20 ° S, and the region equatorward of the jet presents anticyclonic vorticity and

 

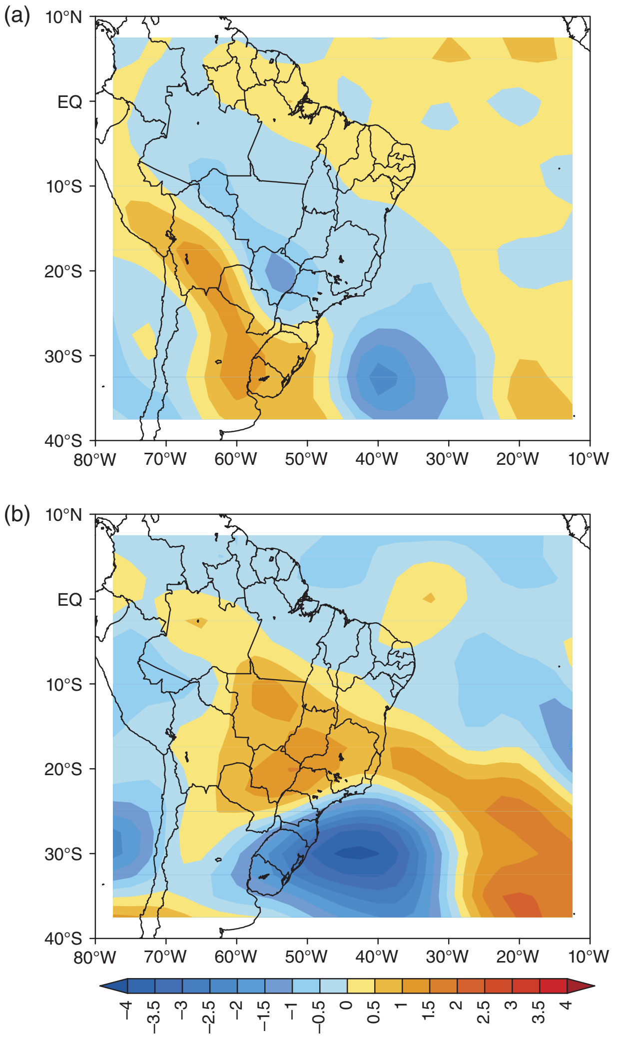


Figure 8. Vorticity anomaly ($10^{-5}$ s$^{-1}$) at 850 hPa (a) and 200 hPa (b) on day *d* for the composites of 16 winter cold front events over the Amazon Basin.

the region poleward of the jet presents cyclonic vorticity over northern Argentina and the adjoining regions of Brazil, Uruguay and Paraguay.

The precipitations and the surface temperatures on days $d-1$ and $d$ and the decline of temperature for the 24 cases are plotted in Figure 13. The precipitation on day *d* varied from around 13 mm in case 20 to 90 mm in case 4, as was previously described. The temperature on day *d* was around 23 °C in most cases except in a few cases when it was below 22 °C. Surprisingly, the correlation between the two variables is a highly insignificant value of −0.01. That is, the temperature, more precisely the minimum temperature, and the precipitation associated with strong cold fronts over the Amazon Basin have no correlation. The wind and humidity distribution and their evolution in the warm air sector determine the intensity of the convective activity and the consequent rainfall during a given event. At Manaus, the CFs produce up to 15 times more rainfall than the daily climatological mean of 5.6 mm day$^{-1}$. The CFs are associated with temperature decline of up to 3 °C from $d-1$ to *d*. The correlation between the temperature decline and the rainfall at Manaus is also insignificant (−0.23). However, the negative correlation indicates that the temperature declines on day *d* after the occurrence of rainfall associated with the CFs. The lack of

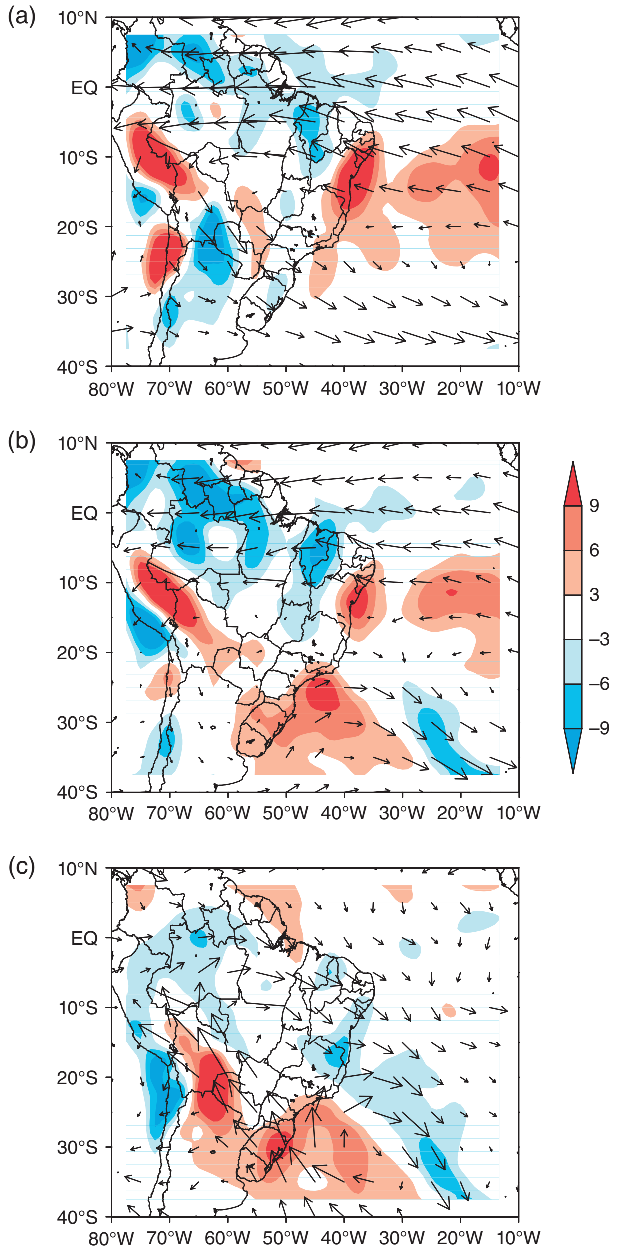


Figure 9. Climatology (a), composites of 16 winter cold front events over the Amazon Basin (b) and anomalies (c) of moisture flux integrated in the vertical (vectors) ($10^3$ m$^2$ s$^{-1}$) and moisture convergence (shades) ($10^{-5}$ s$^{-1}$). Blue: convergence; Red: divergence.

correlation between the precipitation and the temperature may be partially due to the high spatial variability of the convective activity triggered by the cold frontal incursions into the Amazon Basin. This makes forecasting quantitative precipitation in the frontal situations difficult.

The mean thermal structure in the lower and middle tropospheres obtained from the 24 frontal situations is shown in Figure 14. At the surface (1000 hPa) (Figure 14(d)), the penetration of relative cold air into the western portion of the Amazon Basin is evident. The cold air mass is shallow, confined to the layer below 850 hPa. The amplitude of the thermal wave weakens with altitude. At 500 hPa (Figure 14(a)), only a small ripple is seen over eastern Brazil. That is, northward advection of the cold air occurs in the surface layers and over the western parts of the subtropical and tropical South America. The cold fronts

 

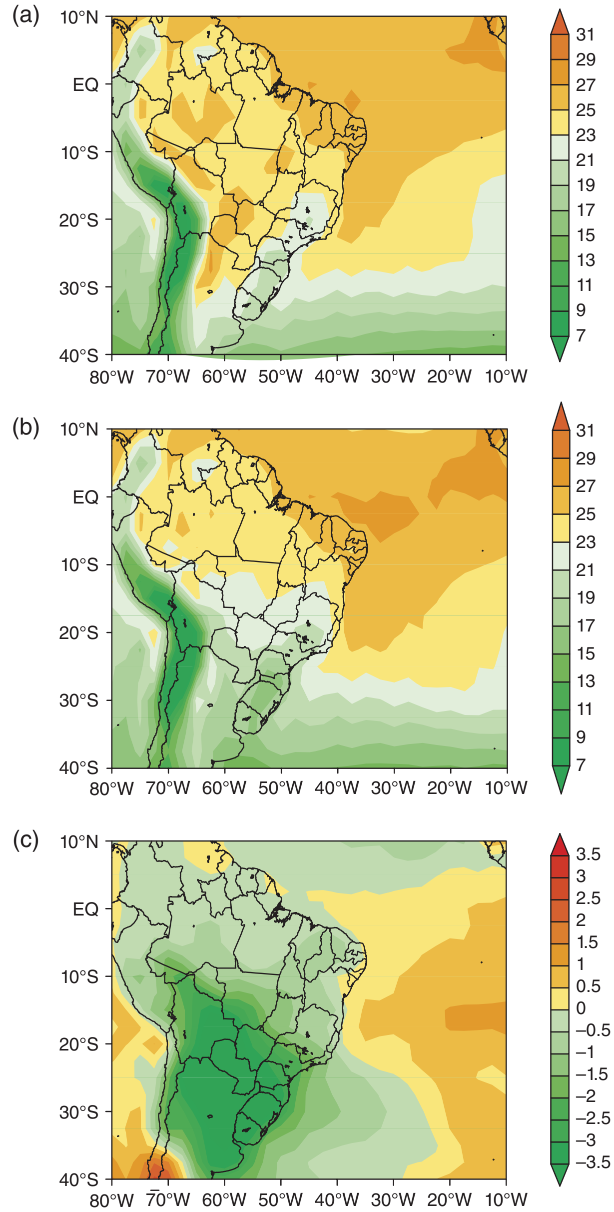


Figure 10. Same as in Figure 4 except for surface temperature composite of eight summer cold front events over the Amazon Basin.

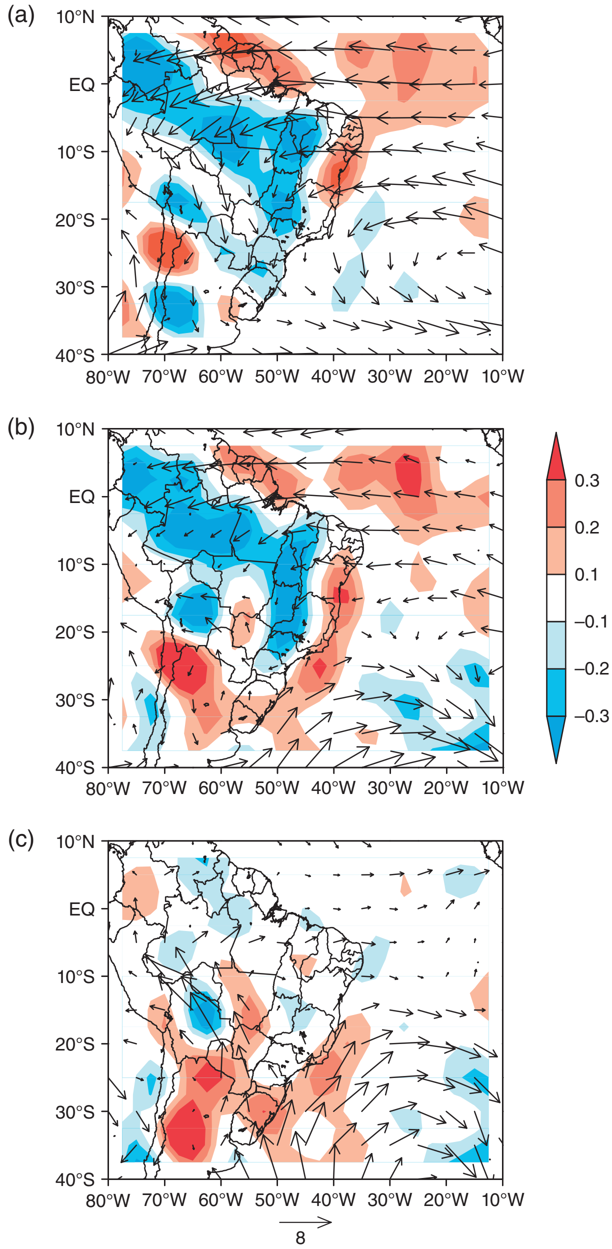


Figure 11. Same as in Figure 5 except for eight summer cold front events.

that affect the Amazon Basin strongly do not affect the surface temperature in northeast Brazil.

### 4.2. Temporal variability of precipitation and temperature: two cold front cases

The individual frontal events may differ substantially from the composite situation described above, especially in terms of local variations of precipitation and temperature. Thus, an interesting evolution is seen of the precipitation, maximum and minimum temperatures and surface pressure during the advance of a cold front from southern Brazil into the Amazon Basin at the three locations shown in Figure 1.

The meteorological variables around day *d* associated with two cold frontal incursions into the central Amazon Basin, cases 24 and 1 listed in Table 1 are plotted in Figures 15 and 16, respectively. Case 24 occurred in austral winter and produced moderate rainfall of about 14 mm on 17 July 2010 at Manaus (Figure 15(a)). Case 1 occurred in summer and produced heavy rainfall of about 72 mm at Manaus (Figure 16(a)). The evolutions of the variables are briefly described below, case by case.

In the austral winter case, heavy rainfall of 42 mm was registered at São Paulo on 14 July 2010 (Figure 15(a)), but Manaus received only about 14 mm 3 days later. Lesser amounts of rainfall were registered on 13 and 15 July, 1 day before and 1 day after the frontal passage on 14 July at São Paulo. The day of the passage of the cold front could be inferred from the steep fall of maximum temperature from 12 to 14 July by about 13 °C (Figure 15(b)). At Brasilia, the maximum temperature fell only slightly by 4 ° C from 14 to 16 July (Figure 15(b)) and the rainfall was small (Figure 15(a)). At Manaus, the maximum temperature fell more steeply, about 8 °C from 16 to 17 July and about 2 °C from 17 to 18 July, than at Brasilia. Clearly, there is a lag of 3 days, in this case, between the cold frontal passages at São Paulo

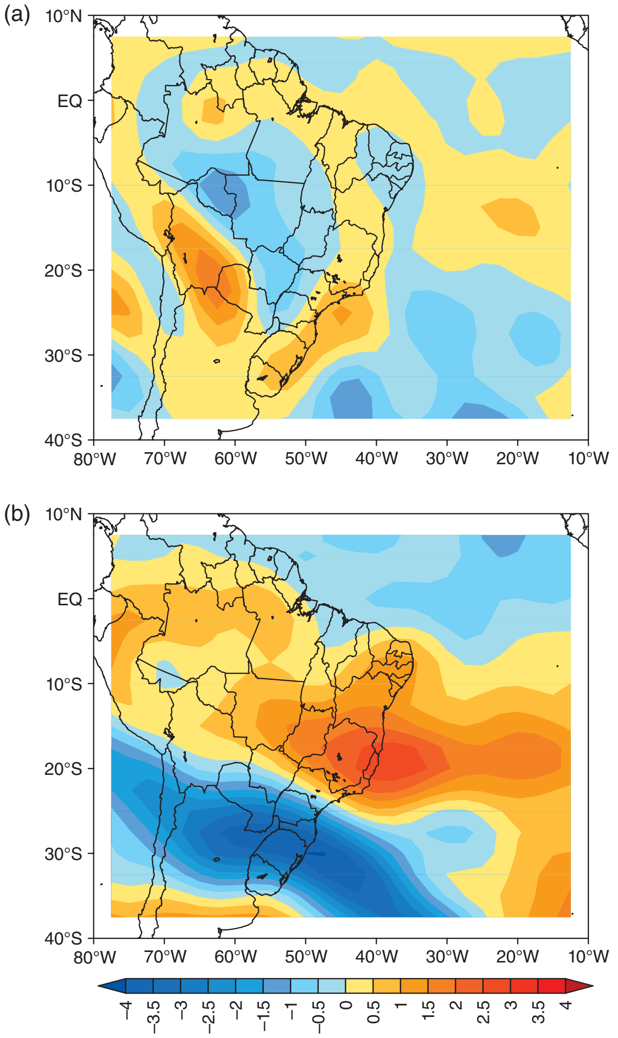


Figure 12. Same as in Figure 8 except for eight summer cold front events.

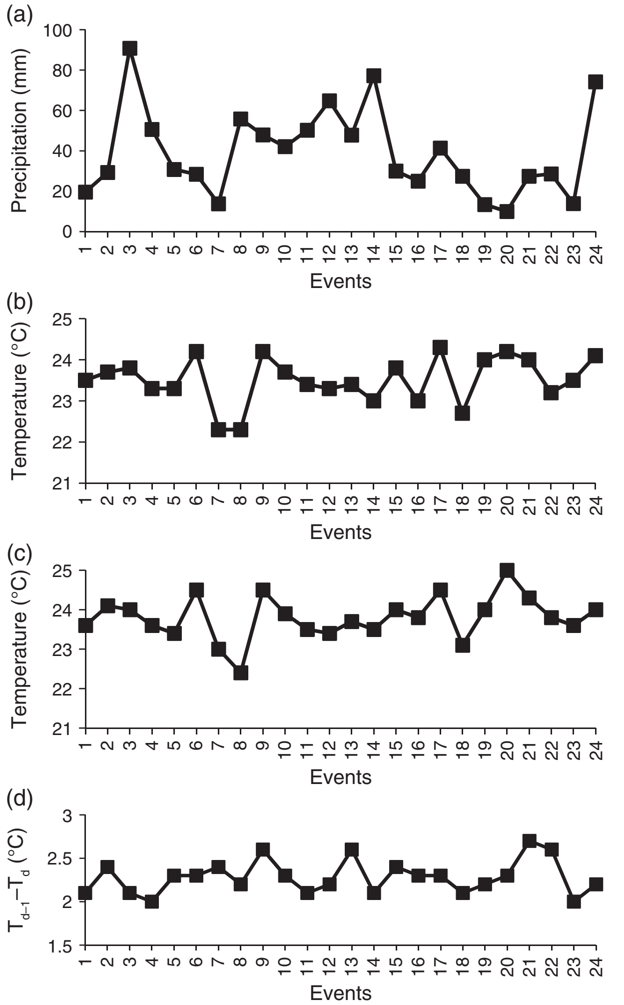


Figure 13. (a) Twenty-four hours precipitation measured on day *d*, (b) temperature on day *d*, (c) temperature on day *d* + 1 and (d) the temperature decline on day *d* with respect to day *d* − 1, for 24 cold front events over the Amazon.

and at Manaus. The cold air mass that affected Manaus must have moved northward close to the Andes, guided by the topography, as seen in Figure 14(d). That is the reason for a smaller decline in temperature at Brasilia, where the prefrontal rainfall was more intense than that on the day of frontal passage. The minimum temperature at São Paulo declined by 5 °C from 12 to 14 July, while there was no change at Brasilia (Figure 15(c)). However, the minimum temperature at Manaus declined gradually from 15 to 18 July by about 5 °C. This case had happened in midwinter and, therefore, the temperature declines were very prominent at São Paulo. In general, the maximum and minimum temperatures at Brasilia and São Paulo are lower than those at Manaus, consistent with the latitude and the elevation of those two stations. The surface pressure at Manaus (Figure 15(d)) showed a small decline from 14 to 15 July but, in general, there was a gradual increase of about 8 hPa from 12 to 19 July. The surface pressure is not a good indicator of the passage of frontal boundary in the central Amazon Basin.

In the summer case also presented in Figure 16, there was a lag between the precipitation peaks at São Paulo and Manaus. However, the lag was only 1 day. In this case, the precipitation at Manaus was many times more intense than that at São Paulo or at Brasilia. There were two cold frontal passages in succession at São Paulo during the period presented, one on 14 and the other on 18 July, with declines in maximum temperature of 9 °C from 12 to 14 July and 7 °C from 17 to 18 July. Manaus registered a decline of 7 °C from 14 to 15 July and 4 °C from 17 to 18 July. The changes in the minimum temperature at São Paulo and Manaus are almost simultaneous, perhaps unrelated to the frontal passage event at Manaus. In this case, although the surface pressure at Manaus showed a decline of about 4 hPa from 11 to 13 July, there was no appreciable change from 13 July to the day of frontal passage on 15 July (Figure 16(d)).

From the two cases of frontal incursions presented, it can be said that at Manaus, the minimum temperature decline is much smaller than the maximum temperature decline and the surface pressure is not a good indicator of frontal passage. There are large seasonal differences in precipitation, being heavy in summer and moderate in winter. The lag between the frontal passages at Manaus and São Paulo decreases from 3 days in winter to 1 day in summer.

### 4.3. Lower tropospheric circulation: two cases of cold front over the Amazon Basin

The near-surface circulation features associated with a cold front over the Amazon Basin, one case each in austral winter

 

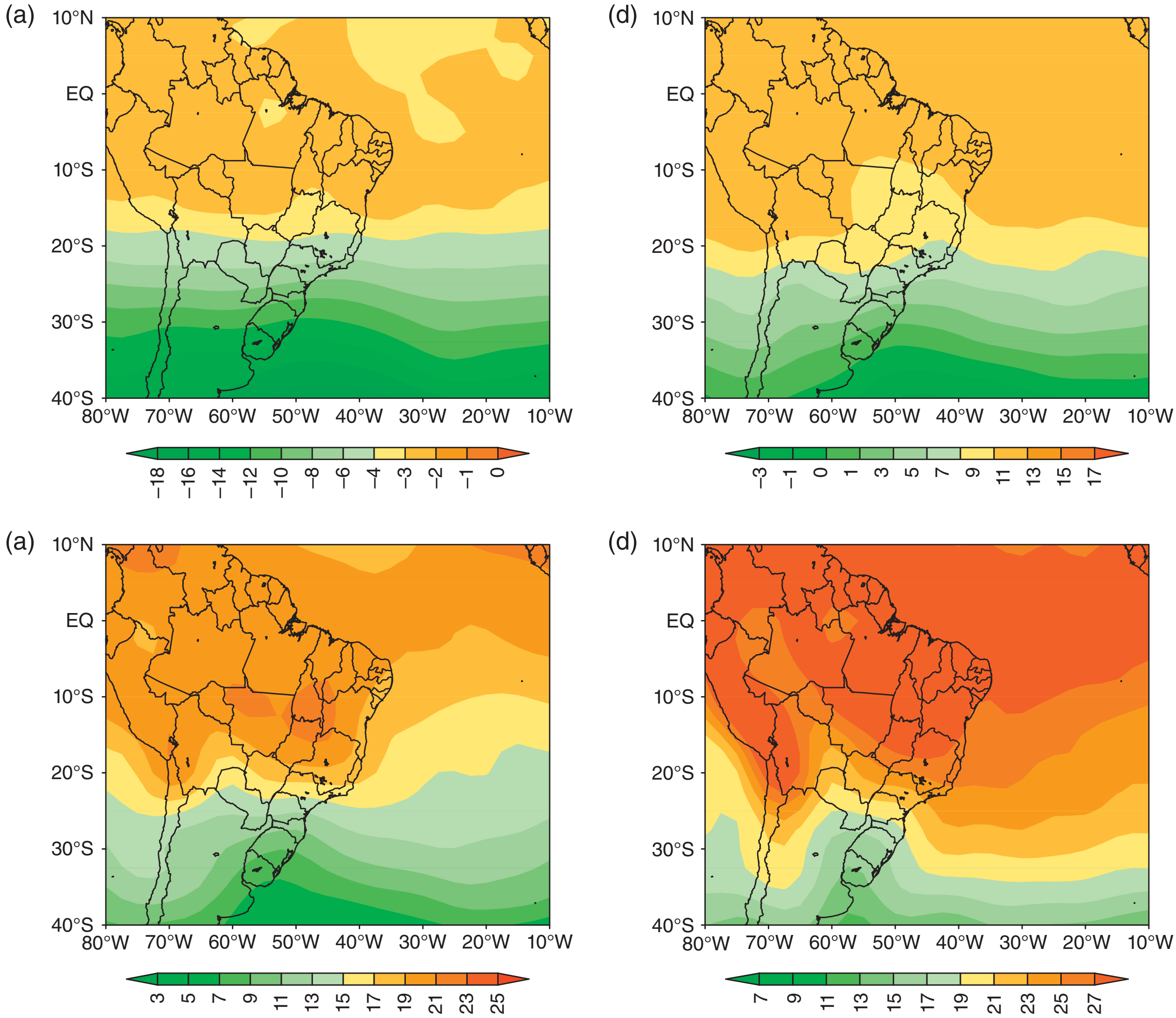


Figure 14. Temperature (°C) composites on day *d* of 24 cold front events over the Amazon Basin. (a) 500 hPa, (b) 700 hPa, (c) 850 hPa and (d) 1000 hPa.

and austral summer, are presented here to appreciate the seasonal differences. Figures 17, 18 and 19 show the 925 hPa geopotential, wind and temperature fields, respectively, and their anomalies with respect to climatology, for the winter case of 17 July 2010 (case 24 of Table 1). On 16 July ($d-1$), the geopotential field (Figure 17(a)) shows a high pressure cell situated over Argentina, Uruguay and the adjacent regions and the low centre associated with the front situated south of 40° S between 30 and 20° W. The cold front situated along the northern fringe of the high pressure area affects the southern parts of the Amazon Basin. It is interesting to observe an inverted trough in the northern flank of the high pressure cell on $d-1$, $d$ and $d+1$ (Figure 17(a–c)). This is characteristic of the cold frontal situations reaching the Amazon Basin in autumn and winter (Satyamurty *et al.*, 2001). The extratropical high and low pressure centres move 13° longitude eastward from 16 to 18 July (from $d-1$ to $d+1$). The inverted trough over the continent does not propagate but deepens on day *d* and weakens later. The same characteristics are seen in the anomaly fields (Figure 17(d–f)).

Strong southerly 925 hPa winds reach north of 10° S over the western parts of the Amazon Basin on 16 July ($d-1$) (Figure 18(a)) advancing north of 10° S over the southern Amazon Basin on day *d* (Figure 18(b,e)), indicating strong cold air advection. The wind anomalies (Figure 18(d–f)) show strong southerlies and cyclonic movement around the inverted trough. West of the inverted trough over the continent, the southerly winds advance into the western and the central Amazon Basin.

The temperature fields at 925 hPa (Figure 19) show cold anomalies advancing north of 10° S from $d-1$ to $d+1$ in the central western parts of the continent. The anomaly fields (d–f) show a clear separation of warm and cold air masses with the frontal boundary oriented northwest–southeast from southern Venezuela to 20° S, 50° W on day *d* (Figure 19(e)).

Figures 20, 21 and 22 show the same flow characteristics for the austral summer case of 15 November 2000 (case 1, Table 1). Development and structure of the fields in this case are basically similar to those described above. However, there are some appreciable differences between the two cases. The inverted trough over southern Brazil is weaker than that in winter, and the eastward movement of the extratropical low and the high geopotential centres is faster (10° longitude *per* day) (Figure 20(a–c)). The southerly winds east of the Andes do

 

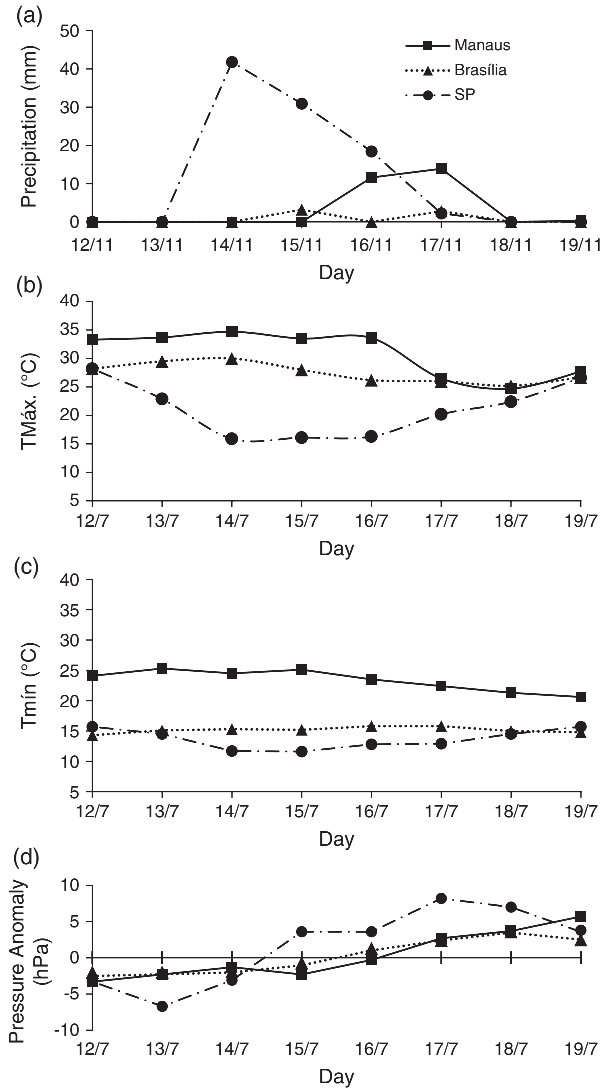


Figure 15. Evolution of meteorological parameters associated with the cold frontal incursion in central Amazon Basin during the period 12–19 July 2010 (Event 24 of Table 1). (a) Precipitation (mm/day), (b) maximum temperature (°C), (c) minimum temperature (°C) and (d) surface pressure (hPa).

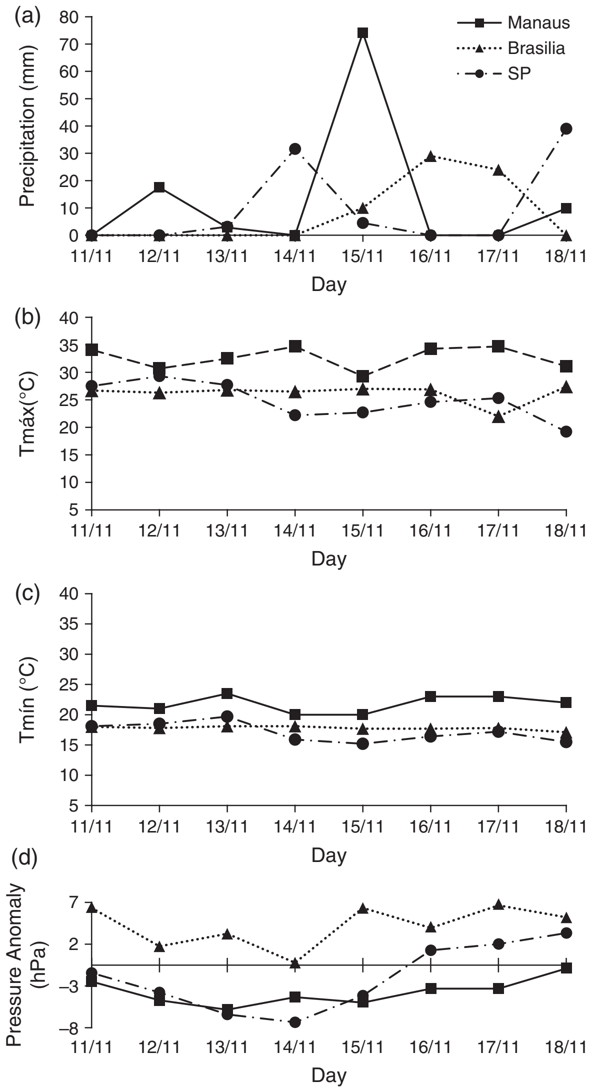


Figure 16. Same as in Figure 15 except for the period 11–18 November 2000 (Event 1 of Table 1).

not penetrate deep into the equatorial latitudes, reaching only up to 10°S in summer (Figure 21(a–c)). The wind anomalies (d–f) over the Amazon Basin on day *d* are westerlies. The negative temperature anomaly (Figure 22(d–f) is felt more over the eastern part of the Amazon Basin than over its western portion.

## 5. Conclusions and discussion

South America, especially the region east of the Andes Mountains, is a region of intense interaction between the tropics and the extratropics, where the cold air masses penetrate as far north as the Amazon Basin (Fortune and Kousky, 1983). From the analysis presented above, the following characteristics about the structure and evolution of cold frontal incursions into the Amazon Basin are obtained. Occasionally (2.3 *per* year) strong cold fronts in terms of temperature decline penetrate into the Amazon Basin from the south, two-thirds of them in austral winter and the remaining in austral summer. These cold fronts affect the basin with intense precipitation (of more than 40 mm day$^{-1}$ on average) and decline in daily maximum temperatures of ~8 °C in 2 days in the southern and central parts of the Amazon Basin. In a cold frontal situation in the Amazon Basin, the transport of moisture from the basin southward is reduced or is absent, thus increasing the convergence of moisture flux over the basin, which is essential for the convective activity that brings the observed rainfall.

In the austral autumn and winter cases, the cold fronts reach Manaus 2 to 3 days after they affect São Paulo. The effects at Manaus in terms of temperature decline are stronger than those at Brasilia, indicating that the cold air mass in these cases propagates northward east of the Andes and west of Brasilia over Bolivia and Mato Grosso state of Brazil to reach the Amazon Basin. The austral summer cases of frontal incursions produce more rainfall than the austral winter cases over the basin, agreeing qualitatively with Garreaud and Wallace (GW). The convective activity over the basin is greatly enhanced during the frontal passage episodes as is inferred from the observed rainfall.

One important finding of the present study is that there is no (significant) correlation between the rainfall intensity and

 

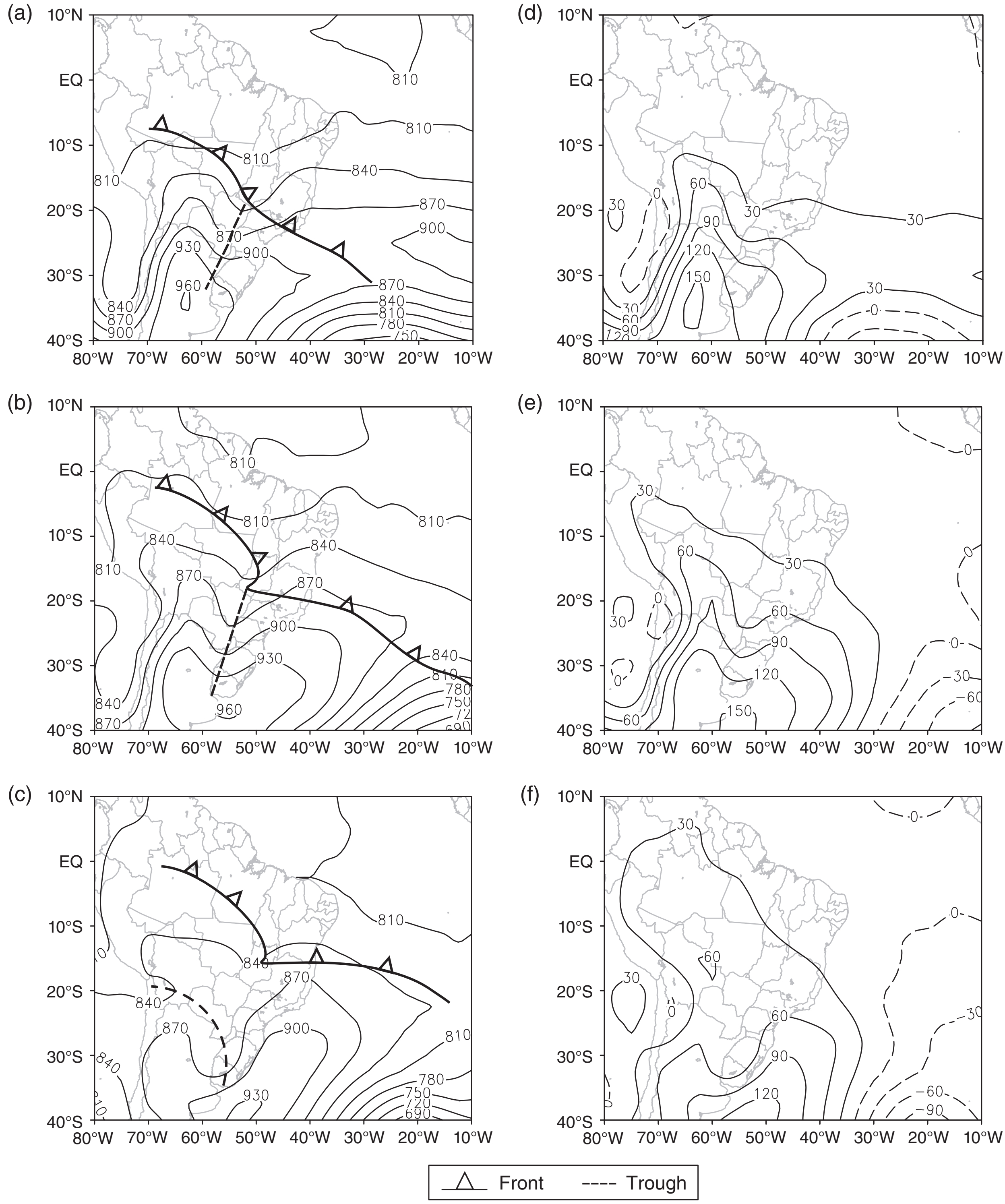


Figure 17. 925 hPa geopotential height (m) on $d-1$ (a and d), on $d$ (b and e) and on $d+1$ (c and f). Left and right columns show observed and anomaly fields, respectively, for Event 24 of Table 1.

the temperature decline associated with cold frontal passages at Manaus. This is probably because in the summer cases the rainfall is high while the temperature decline is low, and the opposite occurs in the winter cases.

The vertical inclination of the extratropical cyclonic centre associated with the cold front is about 12° longitude to the west from the 925 hPa level to the 200 hPa level. That is, the frontal activity over the Amazon Basin is a manifestation of the high-amplitude baroclinic wave in the mid-latitudes of South America and the adjoining oceans. The eastward propagation of the extratropical high and low pressure centres in austral winter (6° $day^{-1}$) is slower than that in summer (10° $day^{-1}$). GW reported a phase speed of 20° $day^{-1}$ for the composite 500 hPa geopotential wave. The differential phase speed of the baroclinic wave between the lower and the upper tropospheres weakens the baroclinity and helps the system to become ultimately

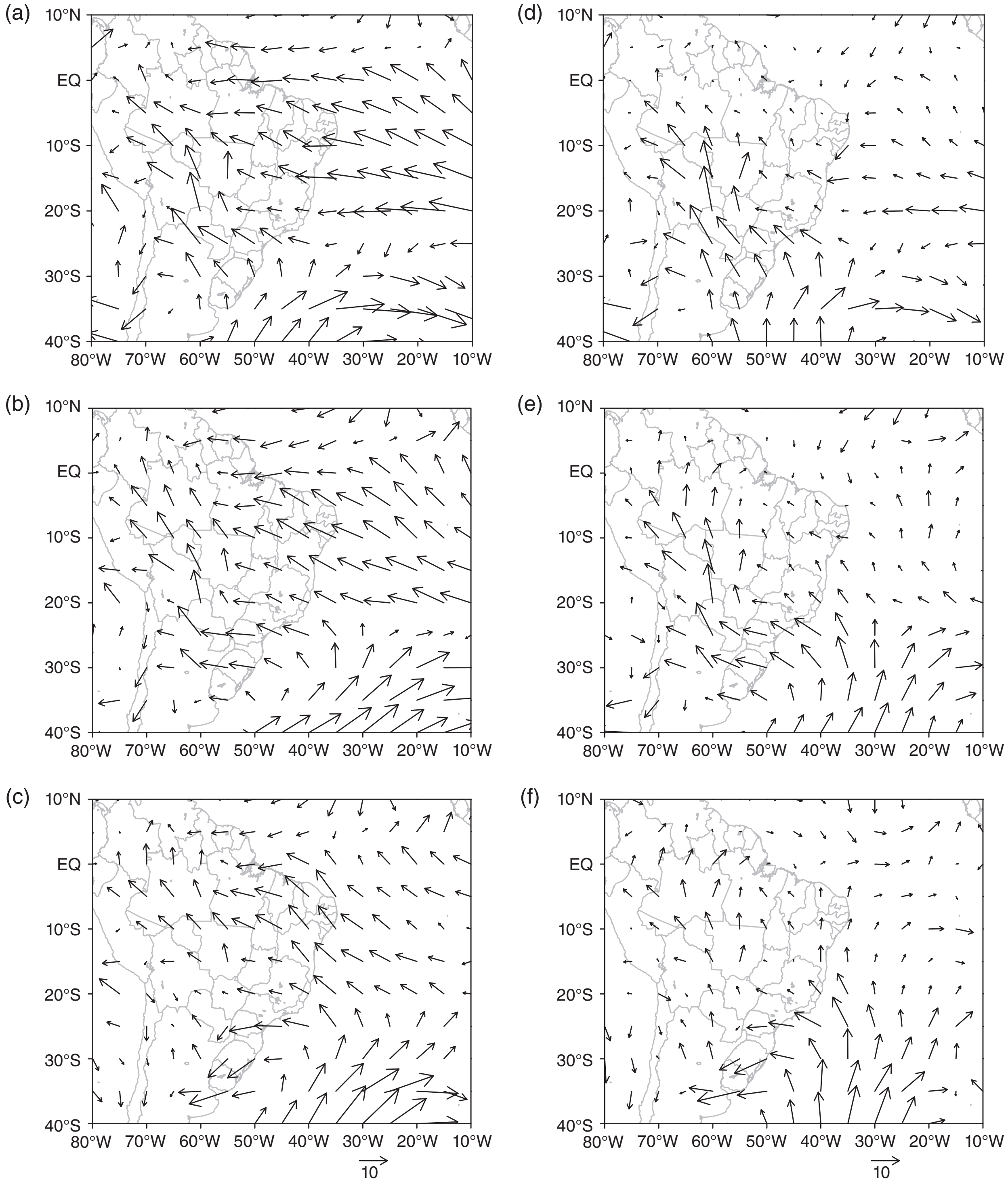


Figure 18. Same as in Figure 17 except for winds (m s$^{-1}$).

barotropic and to dissipate. The meridional movement of the frontal boundary is slower in winter and, therefore, the lag between the frontal passages at Manaus and São Paulo is about 3 days in winter and only 1 day in summer.

A secondary trough forms, especially in winter cases, over the central parts of South America and the southerly winds to its west advect cold air into the Amazon Basin. The effect of the secondary trough pushing strong frontal surfaces into the Amazon Basin was not given importance in the earlier studies of GW and Marengo *et al.* (1997).

Normally the low-level jet (LLJ) flows from the Amazon Basin to the central and southern parts of the continent supplying moisture for the development of convection south of 20° S (Arraut and Satyamurty, 2009). That is, in this part of the globe, the sensible heat and latent heat transfers between the low latitudes and the high latitudes are vigorous. One of the frequently asked questions is what makes this region so special. One immediate answer is the presence of high, narrow and meridionally oriented range of mountains from north of the equator to as far south as 55° S. The mountain acts like a barrier for the equatorial

 

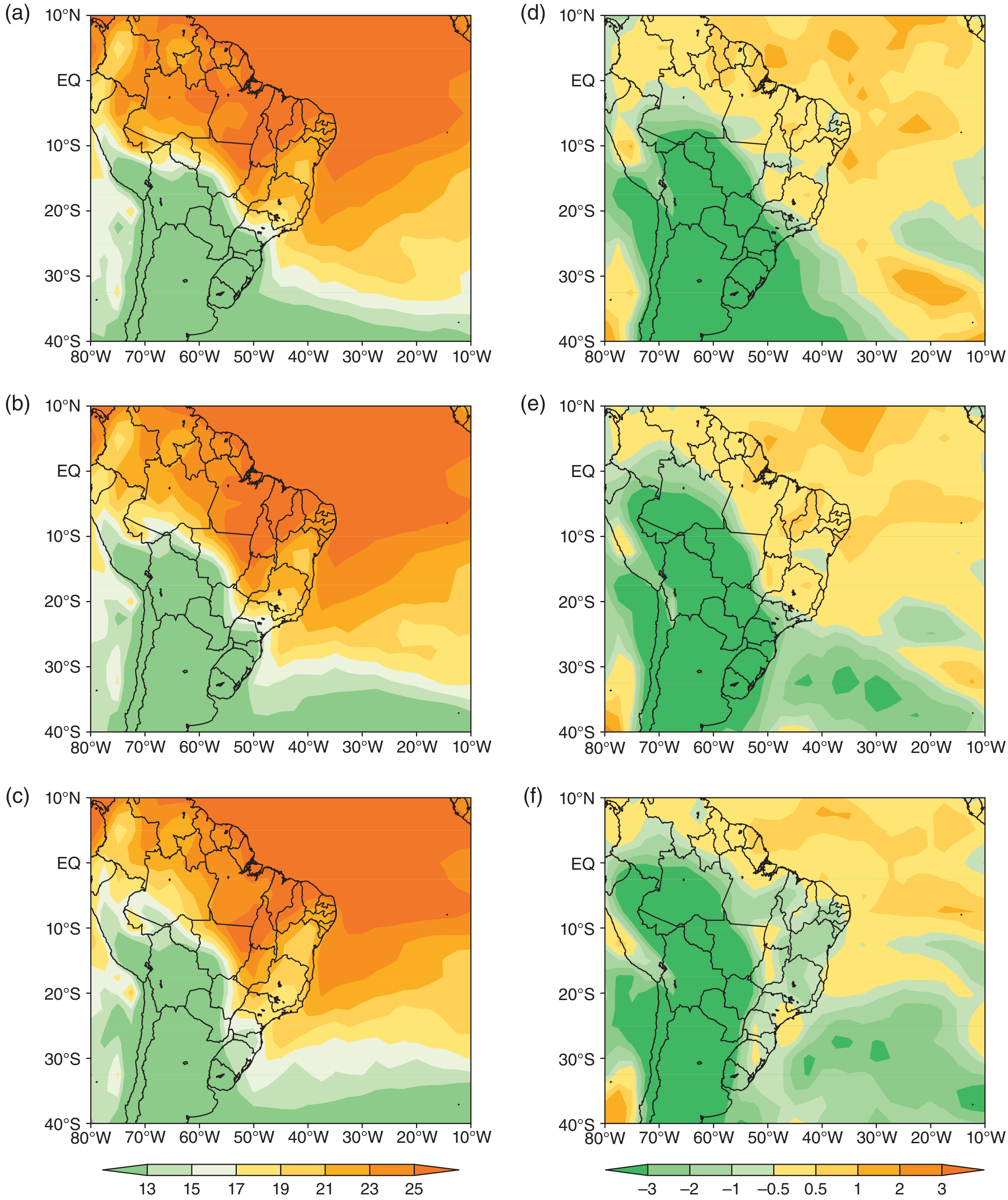


Figure 19. Same as in Figure 17 except for surface temperature (°C). Observed and anomaly fields are given in left and right columns, respectively.

easterlies and the flow turns southward just east of the mountains and the winds present a strong convergence of mass and moisture over the Amazon Basin. The low pressure area over northern Argentina, the Chaco Low, helps the northerly winds to strengthen forming an LLJ (Salio *et al.*, 2002). On the other hand, the westerly flow over the Andes in the mid-latitudes produces a trough near the east coast of southern Brazil (Satyamurty *et al.*, 1981). As a result, the meridional wind components in the middle and the upper portions of the troposphere over the continent are strong southerlies. Thus, the meridional components of winds over the central parts of the continent in the lower troposphere as well as in the upper troposphere are strong, making the interaction between the extratropics and tropics strong in this part of the globe. In this scenario, the cold fronts play an important role in the weather fluctuations over subtropical and tropical South America.

Krishnamurti *et al.* (1999) proposed a mechanism of downstream amplification for the strong frontal boundaries in South

 

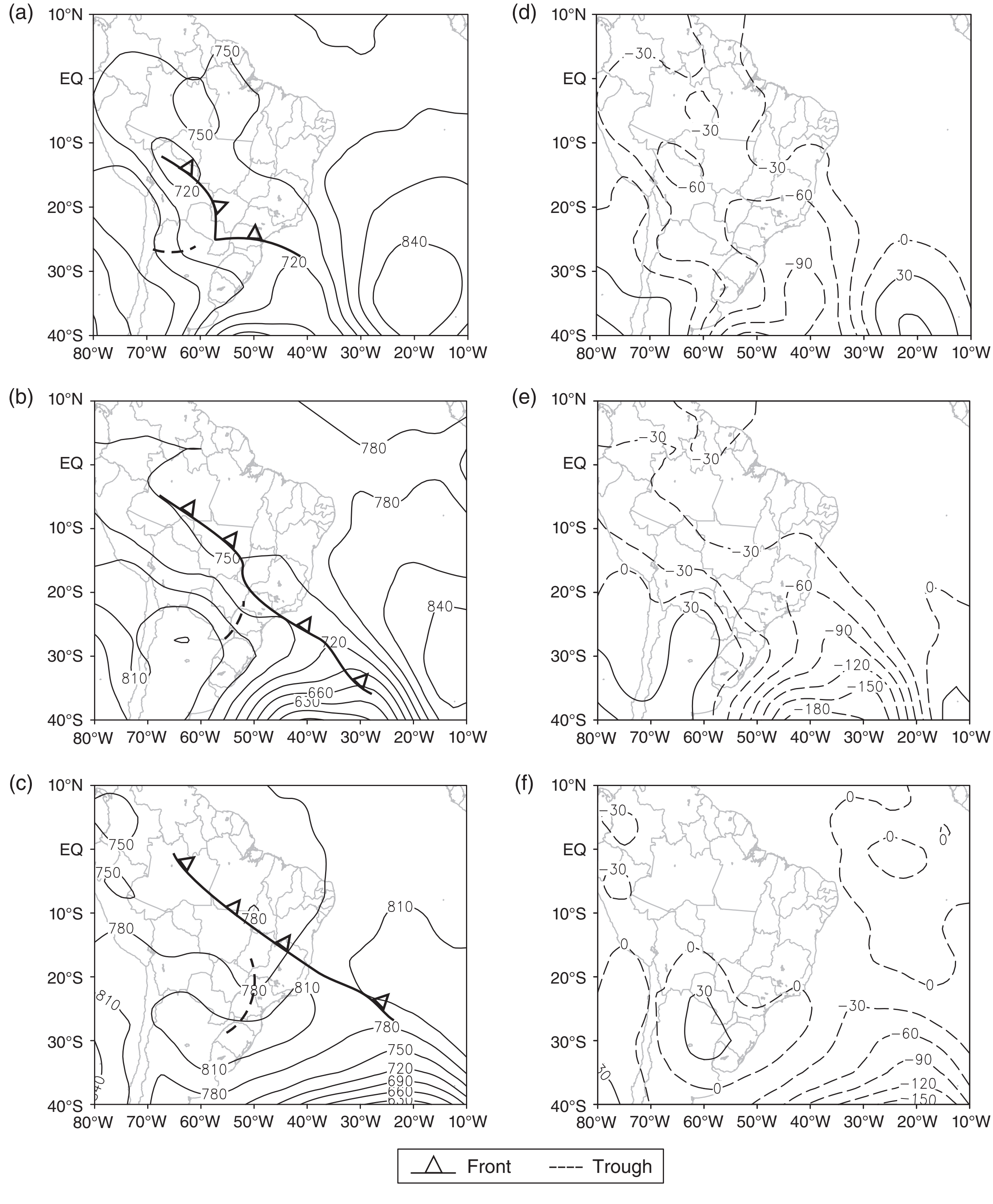


Figure 20. Same as in Figure 17 except for Event 1 of Table 1.

America. The central parts of South America and southeastern Brazil are favoured by frontogenesis because of the deformation field in the winds (Satyamurty and Mattos, 1989). That is, when conditions are suitable, the extratropical perturbations propagating into South America frequently amplify and the associated frontal boundaries strengthen and move northeastward and northward, occasionally affecting the Amazon Basin. The formation of a secondary low centre over the continent in the subtropics, especially in winter situations, seems to be crucial for the cold southerlies to reach the Amazon Basin. Investigation of the mechanisms for the development of this important secondary (subsynoptic-scale) trough on the frontal boundary over the continent makes an interesting study.

The emphasis of the present study is on the temporal variability and the weather associated with strong frontal boundaries reaching the Amazon Basin. The criterion for selecting the cases is based on the intensity of surface temperature changes observed at Manaus in the central parts of the Amazon Basin.

 

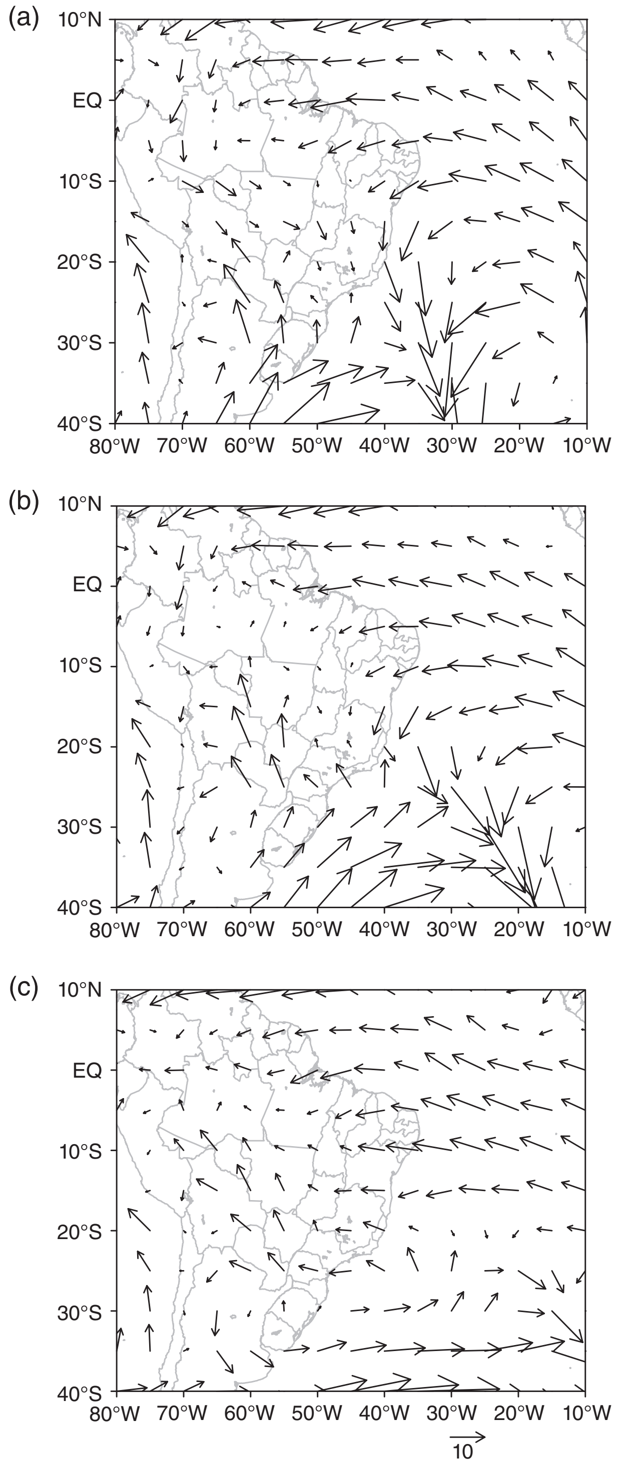


Figure 21. Same as in Figure 17 except for winds for Event 1 of Table 1.

Moisture flux characteristics of the cold frontal situations are important information. The present work complements the work of GW providing information about the differences between winter and summer fronts affecting the Amazon Basin. Although the temperature decline is comparable in the two seasons, the rainfall and its anomaly in the Amazon Basin are heavier in summer.

The cold fronts affecting Northeast Brazil were studied by Kousky (1979). In those situations, the Amazon Basin, especially the western and central portions, are not affected. That is, the northward cold front penetrations over South America are of two distinct types, those affecting the Amazon Basin and those affecting Northeast Brazil (coastal areas). It will be interesting to look into these aspects and identify the conditions for one or the other type to occur.

## Acknowledgements

The authors wish to thank the UEA for the opportunity and encouragement. The second author thanks Dr Maria Gloria de

 

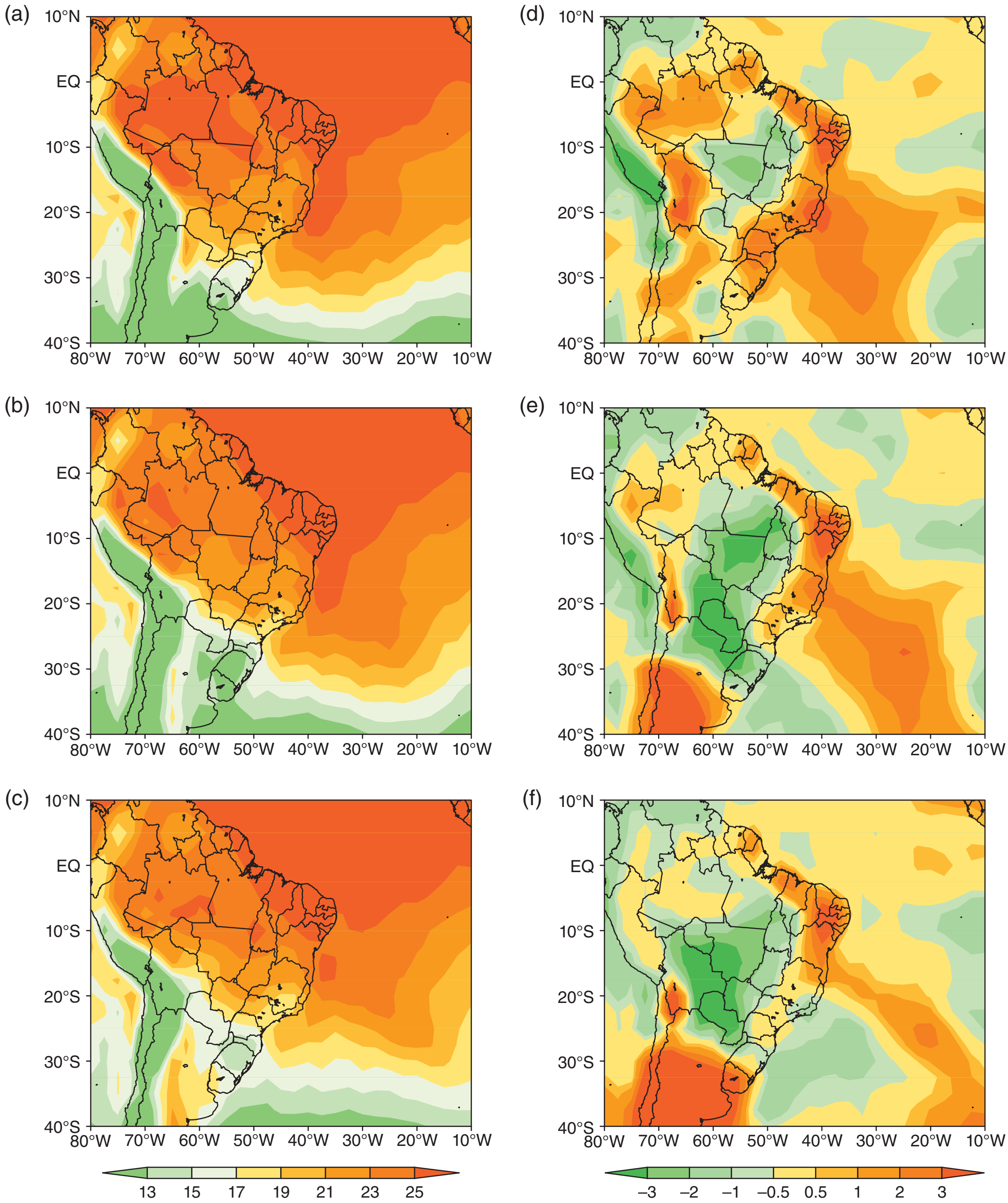


Figure 22. Same as in Figure 17 except for surface temperature for Event 1 of Table 1.

Melo of CESTU, UEA, and Dr Regina Alvalá of CEMADEN for the encouragement and CNPq for the financial support.

## References


Arraut JM, Satyamurty P. 2009. Precipitation and water vapor transport in the southern hemisphere with emphasis on the South American region. *J. Clim.* **48**: 1902–1912.

Bluestein HB. 1993. *Synoptic-Dynamic Meteorology in Midlatitudes. Volume II: Observations and Theory of Weather Systems*. Oxford University Press: Oxford, UK; 608.

Cohen JCP, Silva Dias MAF, Nobre CA. 1995. Environmental conditions associated with Amazonian Squall lines: a case study. *Mon. Weather Rev.* **123**: 3163–3174.

Figueroa SN, Nobre CA. 1990. Precipitation distribution over central and western Tropical South America. *Climanálise* **5**(6): 36–45.

Figueroa SN, Satyamurty P, Silva Dias PL. 1995. Simulation of the summer circulation over the South America Region with an Eta coordinate model. *J. Atmos. Sci.* **52**: 1573–1584.

Fortune M, Kousky VE. 1983. Two severe freezes in Brazil: precursors and synoptic evolution. *Mon. Weather Rev.* **111**: 181–196.

Garreaud RD, Wallace JM. 1998. Summertime incursions of midlatitude air into subtropical and tropical South America. *Mon. Weather Rev.* **126**: 2713–2733.

Kodama Y. 1993. Large-scale common features of subtropical convergence zones (the Baiu frontal zone, the SPCZ and the SACZ). Part II: Conditions of the circulations for generating STCZs. *J. Meteorol. Soc. Jpn.* **71**: 581–610.

Kousky VE. 1979. Frontal influences on Northeast Brazil. *Mon. Weather Rev.* **107**: 1140–1153.

Kousky VE, Ferreira NJ. 1981. Interdiurnal surface pressure variations in Brazil: their spatial distributions origins and effects. *Mon. Weather Rev.* **109**: 2000–2008.


 

Krishnamurti TN, Tewari M, Chakraborty DR, Marengo J, Silva Dias PL, Satyamurty P. 1999. Downstream amplification: a possible precursor to major freeze events over southeastern Brazil. *Mon. Weather Rev.* **127**: 242–270.

Marengo JA, Cornejo AG, Satyamurty P, Nobre CA, Sea W. 1997. Cold surges in tropical and extratropical South America: three strong events in 1994. *Mon. Weather. Rev.* **125**: 2759–2786.

Nogués-Paegle J, Mo KC. 1987. Alternating wet and dry conditions over South America during summer. *Mon. Weather Rev.* **125**: 279–291.

Palmén E, Newton CW. 1969. *Atmospheric Circulation Systems. Their Structure and Physical Interpretation*, International Geophysics Series, Vol. 13. Academic Press: New York and London; 603.

Rao VB, Cavalcanti IAF, Hada K. 1996. Annual variation of rainfall over Brazil and water vapor characteristics over South America. *J. Geophys. Res.* **101**(D21): 26539–26551.

Salio P, Nicolini MN, Saulo C. 2002. Chaco low-level jet events characterization during the austral summer season. *J. Geophys. Res.* **107**: 1–17, DOI: 10.1029/2001JD001315.

Satyamurty P, Costa CPW, Manzi AO. 2013. Moisture source for the Amazon Basin: a study of contrasting years. *Theor. Appl. Climatol.* **111**: 195–209.

Satyamurty P, Fonseca JFB, Bottino MJ, Seluchi M. 2001. An early freeze in central South America in April 1999. *Meteorol. Appl.* **8**: 1–16.

Satyamurty P, Mattos LF. 1989. Climatological lower-tropospheric frontogenesis in the mid-latitudes due to horizontal deformation and divergence. *Mon. Weather Rev.* **117**: 1355–1364.

Satyamurty P, Nobre CA, Silva Dias PL. 1998. South America. In *Meteorology of the Southern Hemisphere*, Karoly DJ, Vicent DG (eds). Meteorological Monographs, **27** (49). American Meteorological Society: Boston, MA; 119–139.

Satyamurty P, Santos RP, Lemes MAM. 1981. On the stationary trough generated by the Andes. *Mon. Weather Rev.* **108**: 510–519.

Vieira SO, Satyamurty P, Andreoli RV. 2012. On the South Atlantic Convergence Zone affecting southern Amazonia in austral summer. *Atmos. Sci. Lett.* **14**: 1–6.

 